Analyst

PAPER

View Article Online
View Journal | View Issue

Cite this: *Analyst*, 2015, **140**, 6071

A miniaturized electrochemical assay for homocysteine using screen-printed electrodes with cytochrome *c* anchored gold nanoparticles†

Thangamuthu Madasamy,* Christian Santschi and Olivier J. F. Martin

Determination of homocysteine (HcySH) is highly beneficial in human physiology and pathophysiology for diagnosis and prognosis of cardiovascular diseases (CVD). Unfortunately, the practicability of the existing methodologies for the determination of HcySH is limited in terms of sample requirements, preparation time and instrumentation cost. To overcome these limitations, we have developed a new miniaturized electrochemical assay for HcySH in which cytochrome *c* (cyt *c*) immobilized on gold nanoparticle (GNP) modified screen printed carbon electrode (SPE) is employed as a biosensing element. The electrochemical characterization of the biosensor (cyt *c*–GNP–SPE) shows quasi-reversible redox peaks at the potentials 0 and −0.2 V, confirming the cyt *c* binding. The methodology of quantification is based on the electrochemical oxidation of HcySH by the Fe^{3+}/Fe^{2+} crevice of cyt *c*, observed at a potential of +0.56 V. Using the amperometric technique, the detection limit of HcySH is found to be 0.3 ± 0.025 μM in the linear range between 0.4 μM and 700 μM, with a sensitivity of 3.8 ± 0.12 nA μM^{-1} cm^{-2}. The practical application of the present assay is validated through the measurement of HcySH in blood plasma samples and the selectivity is ensured by eliminating the impact of the common interfering biological substrates using a Nafion membrane. This biosensor shows striking analytical properties of good repeatability, reproducibility (2.85% SD) and high stability (83% of its initial current response after 4 weeks). This work paves the way for cheap, efficient and reliable point-of-care biosensors for screening one of the major causes of deaths both in the developed and developing countries.

Received 17th April 2015,
Accepted 7th July 2015

DOI: 10.1039/c5an00752f

www.rsc.org/analyst

Introduction

Homocysteine (HcySH) is a potential biomarker of cardiovascular diseases (CVD) including hypertension, coronary heart diseases, stroke and atherosclerosis resulting from the abnormalities in lipoprotein metabolism, oxidative stress and chronic inflammation.[1] Under these conditions, the level of naturally produced HcySH is elevated in blood and becomes essential for the diagnosis and prognosis of CVD.[2] Earlier clinical studies have demonstrated that the increased total plasma HcySH level correlates better than cholesterol with the risk of CVD[3,4] and also proved to be an appropriate analytical tool for the diagnosis of Alzheimer's disease (AD).[5] Recently, the assessment of the HcySH level is used to monitor breast cancer patients during their hormonal treatment with suitable drugs.[6] Further, HcySH is also considered as a biomarker of vitamin B12 (methyl-cobalamine), vitamin B6 and folic acid status due to its important metabolic links with these nutrients.[7] Therefore, there is substantial interest in the development of methods to determine the total HcySH at biologically relevant concentrations.

Direct determination of HcySH is hampered because of the coexisting interfering substrates and hence separation based techniques[8] such as high performance liquid chromatography,[9,10] gas chromatography-mass spectrometry[11] and capillary electrophoresis[12,13] have been commonly used. Despite its good selectivity and low detection limits, it requires extensive, time-consuming sample preparation and derivatization steps prior to sample analysis. Further, optical methods, *viz.* chemiluminescence,[14] fluorescence,[15] and UV-Vis detection protocols,[16,17] which are also employed for clinical HcySH assays, involve expensive reagents and instrumentation systems. To overcome these limitations, electrochemical biosensor techniques have recently been considered as an alternative for the measurement of clinically important biomarkers owing to the obvious practical advantages of operation simplicity (less labor-intensive), low costs of fabrication, and suitability for real time detection.[18–21]

Nanophotonics and Metrology Laboratory (NAM), Swiss Federal Institute of Technology Lausanne (EPFL), CH-1015 Lausanne, Switzerland.
E-mail: madasamy.thangamuthu@epfl.ch; Fax: +41-21-693 24 55;
Tel: +41779980696

†Electronic supplementary information (ESI) available. See DOI: 10.1039/c5an00752f

Hence, there is growing interest in the development of direct and indirect electrochemical methods for the determination of HcySH. Initially, the ability of specific chemicals – for instance aminothiadiazole, nitrogen doped graphene nanosheets and cobalt phthalocyanine modified electrodes – was investigated for the direct oxidation of HcySH.[22–24] Unfortunately, these chemically modified electrodes are kinetically slow, resulting in poor voltammetric responses on conventional electrodes, due to the large oxidation over potential of HcySH. Modifying the electrodes with nanomaterials, *viz.* gold nanoparticles (GNP), carbon nanotubes (CNT) and their combination with mediators to improve the kinetics, leads to a determination of HcySH with improved sensitivity.[25–29] However, the selectivity of these nanomaterial modified electrodes is uncertain and limits their application for real sample analysis. To solve this issue, a new approach based on the nucleophilic addition of thiols to the *o*-quinone (1,4-Michael addition reaction) using catechol as an electrochemical indicator has been recently preferred;[30,31] although it is indirect and additional reagents increase the sample volume and the cost of the analysis. Consequently, a highly specific enzyme modified screen printed electrode (SPE) would be an outstanding approach for the direct measurement of HcySH in miniaturized sample volumes; furthermore, this approach would lend itself into the mass production of electrochemical biosensors at a low cost in comparison with other commonly used electrodes.[32] Using this approach, Ching *et al.* developed a biosensor for HcySH using a D-amino acid oxidase modified SPE,[33] which has potential for fulfilling these requirements but has not yet been tested on biological samples. Hence, there is a real need for the development of a cheap, efficient and reliable point-of-care assay for HcySH.

In the present study we have developed a low cost electrochemical assay for the direct determination of HcySH in one drop of the plasma sample using SPE modified with cytochrome *c* (cyt *c*) anchored gold nanoparticles (GNP) as the biosensing element. Several biosensors have been reported using cyt *c* as the biosensing element for the measurement of hydrogen peroxide, nitrite, nitric oxide, *etc*.[34–36] Moreover, the electrochemistry of cyt *c* over GNP modified electrodes were also investigated for sensor application.[37,38] But, the combination of cyt *c* and GNP for the quantification of HcySH has not been reported yet. To the best of our knowledge, this is the first time that the electrochemical oxidation of HcySH by the Fe^{3+}/Fe^{2+} crevice of cyt *c* is investigated in detail by means of the rate of the reaction, electron transfer coefficient, and diffusion coefficient. The present method is based on the reduction of cyt *c* with thiols in accordance with the earlier report.[39] The modification of SPE with GNP offers a suitable matrix for the binding of cyt *c*, thereby mediating heterogeneous electron transfer between the active site of cyt *c* and the electrode surface. Such a SPE modified with GNP (GNP–SPE) enables nanoampere sensitive measurements with a large linear dynamic range and a low limit of detection. Finally, measurements of HcySH in human plasma samples validate the analytical applicability of the present electrochemical assay.

Experimental

Chemicals and reagents

All the chemicals and reagents were purchased from Sigma-Aldrich (St. Louis, MO, USA) at their highest available purity and used as received without further purification; cyt *c* from bovine heart, L-HcySH, L-methionine (MeSH), L-cysteine (CySH), glutathione (GSH), ascorbic acid (AsA), uric acid (UA), potassium chloride (KCl), potassium nitrate (KNO_3), sodium borohydride ($NaBH_4$), Nafion perfluorinated resin solution, chloroauric acid trihydrate ($HAuCl_4{\cdot}3H_2O$) and 1-ethyl-3-(3-dimethylaminopropyl)carbodiimide (EDC). HcySH solutions were prepared immediately before use. All the solutions were prepared with deaerated 0.1 M PBS (pH 7.2, used as the electrolyte) and doubly distilled water.

Measurement of HcySH in blood plasma samples

A commercially available lyophilized human blood plasma sample was reconstituted in 0.1 M PBS (pH 7.2) and diluted 10 times separately. Then, a 500 μl of the plasma sample was mixed with 500 μl of a 2 M $NaBH_4$ solution which reduces the protein-bound HcySH into free HcySH within 10 min. Then, the determination of HcySH was performed using the amperometric technique by placing 30 μl of the sample over the biosensing element surface. The concentration of HcySH was quantified from the standard addition calibration curve and multiplied by the dilution factor.

Instrumentation

Cyclic voltammetric and amperometric experiments were performed using the CHI 1240B electrochemical workstation (CH Instruments, Austin, USA) with a conventional three electrode system. A three electrode type of SPE (TE100, CH Instruments) consisting of a Ag/AgCl reference electrode, a carbon counter electrode and a carbon working electrode modified with GNP and cyt *c* was used as the biosensing element. The surface area of the working electrode is 0.071 cm^2. The electrode was equilibrated in 0.1 M PBS electrolyte by using cyclic voltammetry until the voltammogram became constant. The morphological scanning electron microscopy (SEM) images and energy dispersive X-ray (EDX) analysis spectra were obtained using a FEI XL30 EBSP SEM and X-ray spectroscopy (Oxford Instruments, UK).

Configuration of the biosensor

Prior to configuration of the biosensor electrode, the SPE was pre-treated as per an earlier report[40] to remove the organic ink constituents or contaminants and to increase the surface functionalities. Briefly, 1 M H_2SO_4 solution was placed over the SPE and the potential was swept from −0.5 to +1.0 V (*vs.* Ag/AgCl) for 10 cycles at a rate of 50 mV s^{-1}. After this pre-treatment, the GNP was electrodeposited on SPE by placing

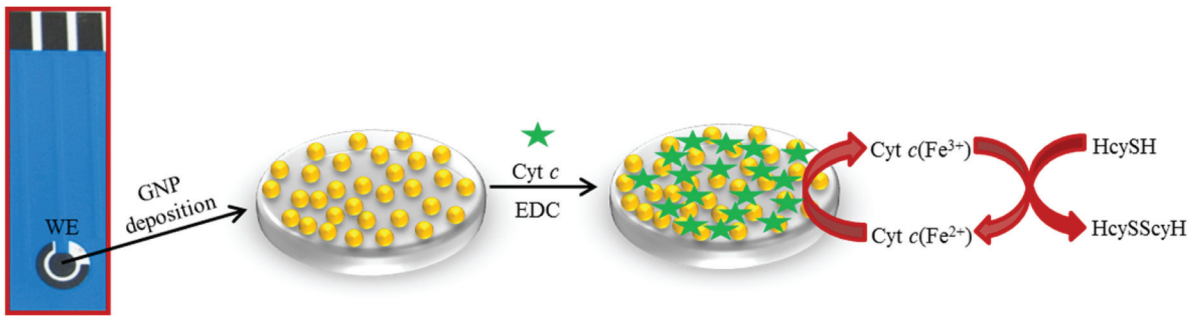

Fig. 1 Schematic representation of the construction of the biosensing element (cyt *c*–GNP–SPE) and illustration of the electrochemical oxidation of HcySH.

the mixture of 0.5 mM $HAuCl_4{\cdot}3H_2O$ and 0.1 M KNO_3 deaerated solutions and cycling the potential from 0.9 to 0 V at a rate of 50 mV s^{-1}. Then, 3 μl of 1 mM cyt *c* solution prepared using 0.1 M PBS was dropped over GNP–SPE and maintained at 25 °C for 5 min. Subsequently, 2 μl of 2 M EDC solution was added to the cyt *c* as a cross linking agent and maintained for 4 h at ambient temperature. During these steps, the positively charged cyt *c* (neutral pH) is electrostatically attached to the negative GNP[41] and forms a stable cyt *c* layer due to the efficient cross linking with EDC (Fig. S1†). Finally, the fully functionalized SPE is immersed in 0.1 M PBS to remove the loosely attached cyt *c* and stored at 4 °C when not in use. Fig. 1 shows the schematic of the biosensor preparation including the electrochemical oxidation of HcySH.

Results and discussion

Direct electron transfer (DET) to or from a deeply buried active site of enzyme to the conducting electrode surface is relatively unique for the development of enzymatic biosensors. Hemoproteins such as quinohemoproteins and cyt *c* containing proteins are able to transfer an electron directly towards electrodes. Among them, quinohemoproteins are mostly preferred for DET because they offer a relatively long and intrinsic electron transfer pathway and they are suitably oriented on the hydrophobic electrode surface which guarantees very good diffusional access of the substrate.[42] However, cyt *c* familiar for biosensing due to its redox behaviour allows measuring the change in the electrochemical signal corresponding to the concentration of the substrates.[43] Even if enzymes are available for DET towards the electrode, in many cases this process is slow due to long electron transfer tunnelling distances. To solve this issue modification of electrodes using suitable nanomaterials has been preferred. In the present work, cyt *c* is used for the biosensing of HcySH and the DET of cyt *c* is enhanced by immobilizing it over GNP which reduces electron transfer distance between SPE and the active site moiety (Fe^{3+}/Fe^{2+}) of cyt *c*.

Morphological characterization

The morphologies of the bare SPE and GNP–SPE were investigated using scanning electron microscopy. As can be seen from Fig. 2, the surface of the bare SPE is porous (Fig. 2a) which may allow more efficient GNP binding. Fig. 2b shows the distribution of ≈40–100 nm sized GNP over the SPE surface. The GNP modified surface provides a suitable environment for the binding of biomolecules, without losing its biological activity and hence this GNP matrix was chosen for the cyt *c* immobilization. Further, energy dispersive X-ray (EDX) spectra of the GNP incorporated SPE shown in Fig. S2† indicate a 7.62% and 69.65% of atomic and weight percentages of GNP.

Electrochemical characterization

The electrochemical behaviors of the bare SPE (curve a), GNP–SPE (curve b) and cyt *c*–GNP–SPE (curve c) were characterized using cyclic voltammetry in 0.1 M PBS (pH 7.2) at a scan rate of 50 mV s^{-1}, as shown in Fig. 3. The voltammograms observed for the bare SPE and GNP–SPE are not showing any characteristic peak but cyt *c*–GNP–SPE shows quasi-reversible redox peaks (separation potential $\Delta E_p = E_{pa} - E_{pc} = 200$ mV, which is greater than 59 mV and $i_c/i_a = 1.36 > 1$) at the potentials of 0 and −0.2 V. Those peaks are characteristic of cyt *c*[44] confirming the attachment of cyt *c* over the GNP–SPE surface. Further, investigations of cyt *c* behavior on the bare SPE also revealed the same characteristic peaks but they were unclear and disappeared at later cycles (data not shown). This may be due to enzyme denaturation and a weak binding mechanism

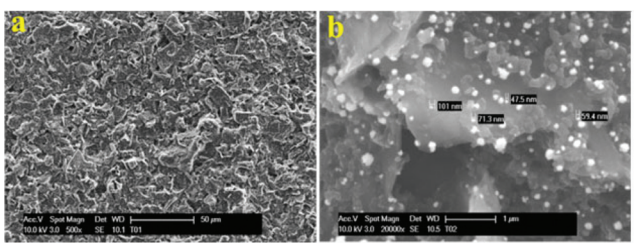

Fig. 2 SEM images of (a) bare SPE (scale bar – 50 μm) and (b) GNP–SPE (scale bar – 1 μm).

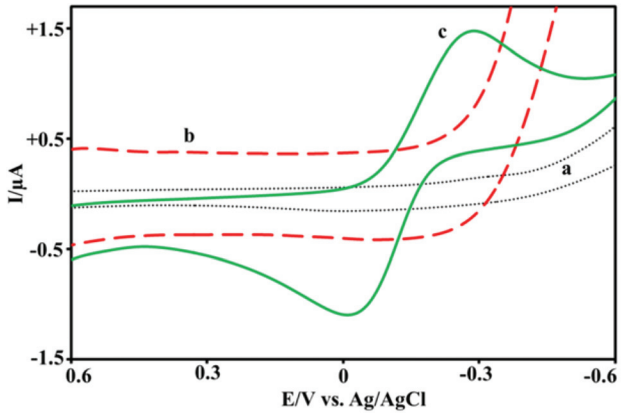

Fig. 3 Typical electrochemical responses obtained for the (a) bare SPE, (b) GNP–SPE and (c) cyt *c*–GNP–SPE in 0.1 M PBS (pH 7.2) at a scan rate of 50 mV s^{-1}.

of cyt *c* on the SPE surface. Furthermore, the effective surface coverage of cyt *c* onto the GNP–SPE was estimated using the Randles–Sevcik equation by measuring the peak intensity of HcySH oxidation:

$$I_p = (2.69 \times 10^5) A n^{3/2} D^{1/2} C \gamma^{1/2}, \quad (3.1)$$

where *C* and *D* are the concentration and diffusion coefficients of HcySH, respectively. The parameters I_p, *n*, γ and *A* correspond to the maximum current response, the number of electrons transferred per molecule, the scan rate and the effective surface area, respectively. The calculated surface coverage of 562.4 nmol cm^{-2} proves the effective binding of cyt *c* to the GNP–SPE surface and the value is related to the surface offered by the spherical shaped GNP (40–100 nm).[45]

Effect of pH

The influence of pH on the activity of the cyt *c* immobilized on GNP–SPE was investigated in the buffered solutions within pH ranging from 3.5 to 8.5 and compared with the results obtained for the cyt *c* on the bare SPE, as shown in Fig. S3.† The maximum response was observed at pH 7.2 in both cases, indicating that the electrocatalytic response is controlled by the activity of cyt *c*. Furthermore, cyt *c* attached to the GNP–SPE (Fig. S3,† curve a) shows a higher current response than on the bare SPE (curve b). This may be due to the better affinity of cyt *c* to the GNP than to carbon, resulting in immobilization of more cyt *c*.[46] An earlier reported strategy[47] indicates that cyt *c* shows its optimum activity at pH 7.0, hence, the present immobilization process does not strongly affect the catalytic function of cyt *c*.

Electrocatalytic oxidation of homocysteine by cyt *c*

The electrochemical oxidation of HcySH on cyt *c*–GNP–SPE and cyt *c*–SPE surfaces was investigated as shown in Fig. 4a in the absence (curves a and b) and presence (curves c and d) of 100 μM HcySH in 0.1 M PBS at a scan rate of 50 mV s^{-1}. Prior to the addition of HcySH, no changes were observed on both

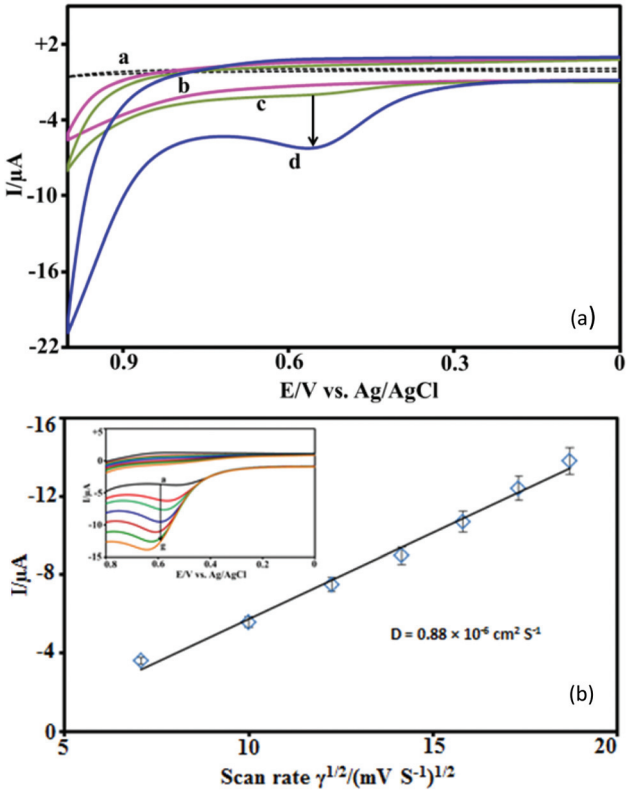

Fig. 4 (a) Electrochemical responses obtained for the cyt *c*–SPE and cyt *c*–GNP–SPE in the absence (curves a and b) and presence (curve c and d) of 100 μM HcySH in 0.1 M PBS at a scan rate 50 mV s^{-1}. (b) Plot of the peak current (*I*) *vs.* square root of the scan rate ($\gamma^{1/2}$) for the 100 μM HcySH in 0.1 M PBS at cyt *c*–GNP–SPE. Inset: typical cyclic voltammograms of the cyt *c*–GNP–SPE for 100 μM HcySH in 0.1 M PBS at various scan rates from (a) 50 to (g) 350 mV s^{-1}.

surfaces, whereas after addition a clear oxidation peak was observed at the potential starting from +0.3 V and extending to +0.6 V, which is in agreement with earlier reports.[48,49] HcySH oxidation occurs due to the electron release from the thiol group in the presence of an electron acceptor cyt *c* as shown in the following equation:

$$2\text{Cyt } c\ (Fe^{3+}) + 2\text{HcySH} \rightarrow \text{HcySScyH} + 2\text{Cyt } c\ (Fe^{2+}) + 2H^+ \quad (3.2)$$

Further, cyt *c*–GNP–SPE (curve d in Fig. 4a) shows a 4 μA higher oxidation current than cyt *c*–SPE (curve c), probably due to the effect of the GNP matrix that offers a suitable environment for the efficient binding of cyt *c* and triggers the electron transfer by reducing the distance between the Fe^{3+}/Fe^{2+} crevice and the electrode surface. In order to verify that the electrochemical oxidation of HcySH at the cyt *c*–GNP–SPE surface is diffusion controlled, cyclic voltammograms for various scan rates (50 mV s^{-1} to 350 mV s^{-1}) were recorded. The resulting oxidation current linearly increased with the square root of the scan rate ($I = -0.8827\gamma^{1/2} + 3.08$, $r^2 = 0.9918$) as shown in Fig. 4b. The slope (0.88×10^{-6} cm^2 S^{-1}) corresponds to the

diffusion coefficient D, *i.e.* the diffusion rate of HcySH molecules towards the surface of the electrode, which is proportional to the concentration gradient (Fick's law). The kinetics of the electrocatalytic oxidation of HcySH by cyt *c* is considered as a pseudo first order reaction due to the constant amount of cyt *c*. The reaction rate was obtained from chronoamperometric data using the Cottrell equation,

$$i = \frac{nFAC_j^0\sqrt{D_j}}{\sqrt{\pi t}} \quad (3.3)$$

where i, n, F, A and t are the oxidation current, number of electrons per molecule, Faraday constant, area of the electrode and time, respectively. The parameters C_j^0 and D_j are the initial concentration and diffusion coefficient of HcySH. This equation simplifies to $i = kt^{-1/2}$, where k is the rate constant. The average k value was found to be 23.95 ± 3.69 M s^{-1} using the slope of the current (i) *vs.* $t^{-1/2}$ plots, obtained for various concentrations of HcySH (Fig. S4†). Furthermore, the nature of the electrochemical reaction between HcySH and cyt *c* was also verified by determining the electron transfer coefficient (α) which is a measure of the energy barrier symmetry. In the present investigations, the value of α is found to be 0.296 using the slope of the Tafel plot ($2.303RT/\alpha nF$) as shown in Fig. S5,† strongly confirming the oxidation. In addition, this value also suggests that the transition state is formed close to the reactant side (α values less than 0.5 are transition states close to the reactant side whereas for transition states close to the product side the α values are higher than 0.5).[50]

Amperometric determination of homocysteine

In order to determine the optimum operating potential for the measurement of HcySH, the anodic current dependency on the applied potential was investigated with time based amperometry for different constant potentials. As shown in Fig. 4a (curve d), the oxidation signal gradually increased from +0.3 to +0.56 V and reaches a maximum at +0.56 V. Therefore, the performance of the biosensing element (cyt *c*–GNP–SPE) for various concentrations of HcySH was investigated using the amperometric technique by applying a constant potential of +0.56 V as shown in Fig. 5a. A linear increase in the oxidation current with increasing HcySH concentration was observed in the amperograms (current *vs.* time) and the observed anodic currents *vs.* HcySH concentrations were plotted as depicted in Fig. 5b (the inset represents a linear calibration curve over the whole range). The obtained calibration curve exhibits a dynamic linear range over the concentration of HcySH from 0.4 μM to 700 μM with a detection limit of 0.3 ± 0.025 μM and a sensitivity of 3.8 ± 0.12 nA μM^{-1} cm^{-2}. These values are comparable to the earlier reported methods as shown in Table 1.

Specificity

Since the oxidation potential of HcySH is positive and relatively high, other electroactive species such as ascorbic acid (AsA) and uric acid (UA) present in the blood plasma would also be oxidized and interfere with the measurements. Structurally similar amino acids are also suspected for altering the current response. So, it is essential to study possible interferences for the selective measurement of HcySH. To investigate the selectivity of the assay, the change in the oxidation current was observed upon the addition of 100 μM of each interfering substrate with 100 μM HcySH. An addition of 100 μM UA did not alter the current response, confirming that UA does not interfere with the measurement. Nevertheless, addition of AsA steeply reduced the current response as shown in Fig. 6, due to the strong reducing property of AsA converting the ferric heme group of cyt *c* (Fe^{3+}) into the ferrous form (Fe^{2+}) and subsequently cyt *c* loses its activity for the oxidation of HcySH. In order to eliminate the interference due to AsA, the biosensing element (cyt *c*–GNP–SPE) was covered with a Nafion membrane[52] by placing the Nafion resin solution (5% solution

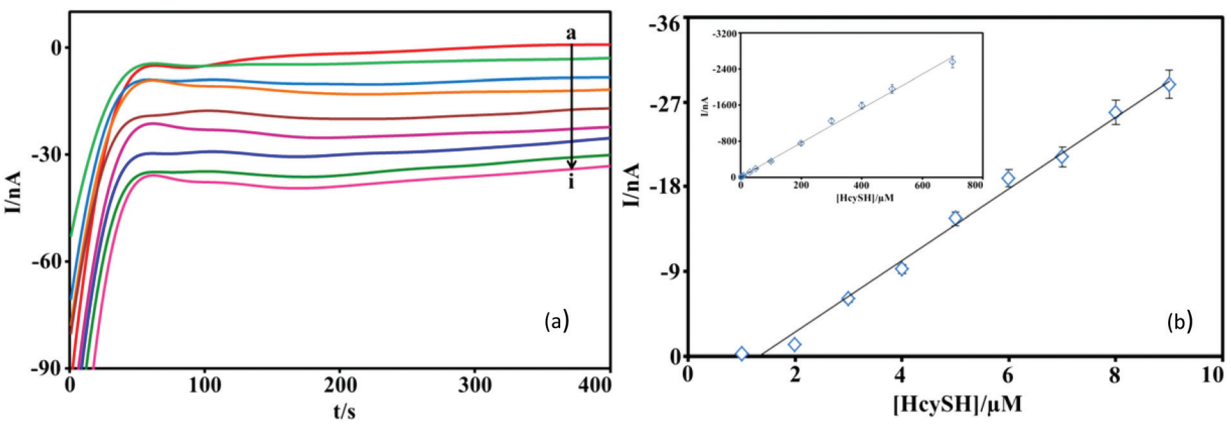

Fig. 5 (a) Typical amperometric time *vs.* current responses of the cyt *c*–GNP–SPE in 0.1 M PBS containing (a) 1 μM, (b) 2 μM, (c) 3 μM, (d) 4 μM, (e) 5 μM, (f) 6 μM, (g) 7 μM, (h) 8 μM, (i) 9 μM of HcySH at a fixed potential of +0.56 V. (b) Linear calibration plot of the anodic oxidation current *vs.* HcySH concentrations in the range of 1–9 μM of ($y = -3.815x + 5.0519$, $r^2 = 0.9921$). Inset: the linear calibration plot of the anodic oxidation current *vs.* HcySH concentrations in the range of 0.4–700 μM ($y = -3.81x - 5.848$, $r^2 = 0.9966$). Each point represents the average value over three measurements.

Table 1 Comparison of the electroanalytical parameters of the present electrochemical assay with earlier reported biosensors

Sensing elements	Linearity (μM)	Sensitivity (μA μM^{-1} cm^{-2})	Detection limit (μM)	Reference
CNT/SPE	1–10	0.2 ± 0.02	0.660 ± NR	Lee *et al.* (2014)[30]
CNT/GCE[a]	2.5–1000	NR[f]	0.89 ± 3.53	Salehzadeh *et al.* (2014)[31]
MWCNT/CPE[b]	5–800	NR	3.3 ± NR	Fouladgar *et al.* (2014)[49]
MnO_2/SPE	5–80	NR	0.47 ± NR	Liano *et al.* (2008)[51]
p-ATD[c]/GCE	0.1–1.4	0.24 ± NR	0.051×10^{-3} ± NR	Kalimuthu *et al.* (2010)[22]
PGE[d]	2–20	NR	1.21 ± NR	Eksin *et al.* (2014)[48]
D-AOx[e]/SPE	6.4–100	0.029 ± NR	6.4 ± NR	Ching *et al.* (2011)[33]
Cyt *c*/GNP/SPE	0.4–700	$(3.8 \pm 0.12) \times 10^{-3}$	0.3 ± 0.025	Present work

[a] Glassy carbon electrode. [b] Carbon paste electrode. [c] Polymerized film of 2-amino-1,3,4-thiadiazole. [d] Pencil graphite electrode. [e] D-Amino acid oxidase. [f] Data not reported.

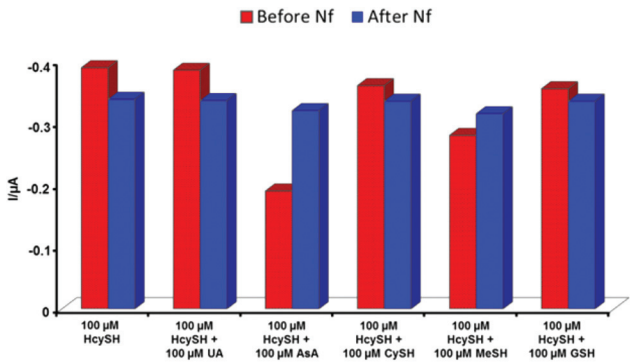

Fig. 6 Histograms representing the oxidation current obtained for the cyt *c*–GNP–SPE before and after Nafion membrane coating, upon addition of 100 μM of UA, AsA, CySH, MeSH and GSH in 0.1 M PBS containing 100 μM HcySH.

(w/w) diluted to a final concentration of 1% (w/w) using ethanol) onto the substrate and drying at room temperature, which resulted in a thin, porous and negatively charged membrane. After Nafion coating, the interference with AsA was eliminated, as indicated by the enhanced oxidation current as shown in Fig. 6. In addition this membrane also reduces the fouling of the biosensor electrode caused by non-specific adsorption of proteins and other molecules typically present in biological samples. Furthermore, the interference with structurally similar thiol compounds such as cysteine (CySH), glutathione (GSH) and methionine (MeSH) was investigated and found that the CySH and GSH were producing negligible changes in the current, Fig. 6. However, the presence of MeSH considerably alters the oxidation current but it can be eliminated by oxidizing into disulfide using hydrogen peroxide[53] (100 μM) prior to the HcySH measurement. The utilization of the Nafion membrane slightly reduces the overall oxidation current due to the lower rate of diffusion of HcySH towards the sensing element.

Stability, repeatability and reproducibility

Long term storage and operational stability are important for the continuous measurements of HcySH over long periods. It was evaluated by monitoring the current response for 10 subsequent measurements in the presence of 10 μM HcySH while the rest of the time it was stored at 4 °C and after 24 h again subjected to the same repetitive measurements. Both sets of experiments exhibit no appreciable changes in the oxidation potential and the peak current inferred from the coefficient of variation (0.45 and 0.52%) which means that the biosensor is stable, not affected by the oxidation products, and can be used for repeatable series of measurements. Nevertheless, for very long term storage, the current response was reduced to 83% after 1 month and 67% after 2 months, as shown in Fig. 7. Further, to ensure a good reproducibility of the experimental results, four biosensors were configured and the magnitude of the current response towards the oxidation of 10 μM HcySH shows among them a SD of 2.85%, which confirms that the measurements are highly reproducible.

Real sample analysis

In common human blood plasma, the HcySH can be found in different forms, *viz.* free or reduced form (contributing for 1–2%), while low-molecular weight disulfides and mixed disulfides contribute to about 10–30% and protein-disulfide coupled HcySH with about 70–80%.[54] Protein-bound HcySH represents a further difficulty for reliable and automated measurements. Hence, the total HcySH, *i.e.* the sum of afore-

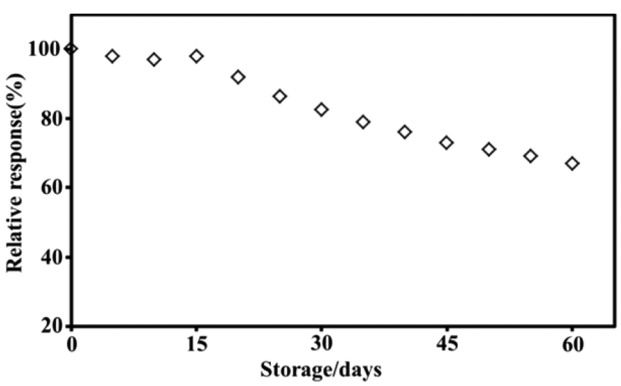

Fig. 7 Relative oxidation current response of the cyt *c*–GNP–SPE over very long term storage.

Table 2 Measurement of HcySH in human blood plasma samples

Human blood plasma	HcySH added (μM)	HcySH found (μM)	Recovery (%)	RSD (%)
Sample 1	10	10.13	101.3	2.1
Sample 2	20	18.63	93.15	1.8
Sample 3	30	27.84	92.60	2.3
Sample 4	40	41.16	102.9	2.0
Sample 5	50	47.85	95.70	1.9

mentioned HcySH species present in the plasma, becomes an essential clinical parameter of interest. In the present assay, the concentration of the total HcySH was quantified using a standard addition technique in the human plasma after reducing it with $NaBH_4$. A drop of the sample was placed on the Nafion membrane covered biosensing element and the corresponding current responses were observed in amperograms. The concentration of HcySH was quantified for each addition, as shown in Table 2, by interpolating the current response into the calibration curve. Each reading represents the average of three measurements. The accuracy of the present assay was tested by determining the recovery of known amounts of HcySH added to the real samples. The good recovery values from 92.6% to 102.9% indicate a good accuracy. The HcySH concentration in the examined plasma sample was found to be 8.5 ± 1.62 μM, indicating that the commercial sample was withdrawn from normal human subjects inferred from the clinically reported normal range (5–16 μM). This value is in good agreement with earlier reported colorimetric methods.[55] The dynamic linear range of the biosensing element suggests its applicability for the hyperhomocysteinemia range, *i.e.* moderate (16–30 μM), medium (30–100 μM) and severe (>100 μM) and hence the present electrochemical assay can potentially be used for point-of-care HcySH measurements.

Conclusion

An electrochemical assay for the direct determination of HcySH concentrations has been successfully demonstrated with a new approach based on the electrochemical oxidation of HcySH using cyt *c* anchored GNP modified SPE. The resulting current corresponds to the concentration of HcySH. The observed kinetic parameters strongly support the methodology of the assay and allow measurements of HcySH in a wide spectrum of concentrations, with a low limit of detection. Further, binding of cyt *c* onto the GNP matrix offers DET by reducing the electron transfer distance between the active site of cyt *c* and the electrode surface which results in measurements with a sensitivity in the nA range. The selectivity of this assay towards biological samples was ensured by eliminating the suspecting interfering substrates using a Nafion membrane. Finally, the analytical applicability of the assay was validated for human plasma samples and the obtained results were in good agreement with standard methods. We conclude that the present electrochemical assay can be highly beneficial towards quality health care management and could be adapted to be part of a point-of care diagnosis of CVD.

Acknowledgements

Thangamuthu Madasamy gratefully acknowledges funding from a Swiss government excellence Post-doc scholarship. We are grateful to C. Brisken for stimulating discussions.

References

1 H. Refsum and P. M. Ueland, *Annu. Rev. Med.*, 1998, **49**, 31–62.
2 R. Clarke, S. Lewington and M. Landray, *Kidney Int.*, 2003, **63**, 131–133.
3 Y. Ozkan, E. Ozkan and B. Simsek, *Int. J. Cardiol.*, 2002, **82**, 269–277.
4 A. S. Wierzbicki, *Diab. Vasc. Dis. Res.*, 2007, **4**, 143–150.
5 D. Press, *Neuropsychiatr. Dis. Treat.*, 2014, **10**, 1887–1896.
6 J. Lin, I. M. Lee, Y. Song, N. R. Cook, J. Selhub, J. E. Manson, J. E. Buring and S. M. Zhang, *Cancer Res.*, 2010, **70**, 2397–2405.
7 D. Faeh, A. Chiolero and F. Paccaud, *Swiss Med. Wkly*, 2006, **136**, 745–756.
8 M. Isokawa, T. Kanamori, T. Funatsu and M. Tsunoda, *J. Chromatogr., B: Anal. Technol. Biomed. Life Sci.*, 2014, **964**, 103–115.
9 B. Frick, K. Schrocksnadel, G. Neurauter, B. Wirleitner, E. Artner-Dworzak and D. Fuchs, *Clin. Chim. Acta*, 2003, **331**, 19–23.
10 R. Accinni, J. Campolo, S. Bartesaghi, G. De Leo, C. Lucarelli, C. F. Cursano and O. Parodi, *J. Chromatogr., A*, 1998, **828**, 397–400.
11 A. Valerio, G. Baldo and P. Tessari, *Rapid Commun. Mass Spectrom.*, 2005, **19**, 561–567.
12 E. Causse, N. Siri and H. Bellet, *Clin. Chem.*, 1999, **13**, 412–414.
13 S. A. Pasas, N. A. Lacher, M. I. Davies and S. M. Lunte, *Electrophoresis*, 2002, **23**, 759–766.
14 X. Mu, S. Zhao, Y. Huang and F. Ye, *J. Sep. Sci.*, 2011, **35**, 280–285.
15 D. W. Jacobsen, V. J. Gatautis and R. Green, *Anal. Biochem.*, 1989, **178**, 208–214.
16 W. Wang, J. O. Escobedo, C. M. Lawrence and R. M. Strongin, *J. Am. Chem. Soc.*, 2004, **126**, 3400–3401.
17 J. O. Escobedo, W. Wang and R. M. Strongin, *Nat. Protoc.*, 2006, **1**, 2759–2762.
18 T. Madasamy, M. Pandiaraj, M. Balamurugan, K. Bhargava, N. K. Sethy and C. Karunakaran, *Biosens. Bioelectron.*, 2014, **52**, 209–215.
19 T. Madasamy, M. Pandiaraj, M. Balamurugan, S. Karnewar, A. R. Benjamin, K. A. Venkatesh, K. Vairamani,

S. Kotamraju and C. Karunakaran, *Talanta*, 2012, **100**, 168–174.
20 T. Madasamy, M. Pandiaraj, A. K. Kanugula, S. Rajesh, K. Bhargava, N. K. Sethy, S. Kotamraju and C. Karunakaran, *Adv. Chem. Lett.*, 2013, **1**, 2–9.
21 M. Pandiaraj, T. Madasamy, P. N. Gollavilli, M. Balamurugan, S. Kotamraju, V. K. Rao, K. Bhargava and C. Karunakaran, *Bioelectrochemistry*, 2013, **91**, 1–7.
22 P. Kalimuthu and S. A. John, *Bioelectrochemistry*, 2010, **79**, 168–172.
23 P. Kannan, T. Maiyalagan, N. G. Sahoo and M. Opallo, *J. Mater. Chem. B*, 2013, **1**, 4655–4666.
24 C. D. Kuhnline, M. G. Gangel, M. K. Hulvey and R. S. Martin, *Analyst*, 2006, **131**, 202–207.
25 L. Agui, C. Pena-Farfal, P. Yanez-Sedeno and J. M. Pingarron, *Talanta*, 2007, **74**, 412–420.
26 F. Gholami-Orimi, F. Taleshi, P. Biparva, H. Karimi-Maleh, H. Beitollahi, H. R. Ebrahimi, M. Shamshiri, H. Bagheri, M. Fouladgar and A. Taherkhani, *J. Anal. Methods Chem.*, 2012, **2012**, 1–7.
27 K. Gong, Y. Dong, S. Xiong, Y. Chen and L. Mao, *Biosens. Bioelectron.*, 2004, **20**, 253–259.
28 V. W. Hung and K. Kerman, *Electrochem. Commun.*, 2011, **13**, 328–330.
29 N. S. Lawrence, R. P. Deo and J. Wang, *Talanta*, 2004, **63**, 443–449.
30 P. T. Lee, D. Lowinsohn and R. G. Compton, *Analyst*, 2014, **139**, 3755–3762.
31 H. Salehzadeh, B. Mokhtari and D. Nematollahi, *Electrochim. Acta*, 2014, **123**, 353–361.
32 Z. Taleat, A. Khoshroo and M. Mazloum-Ardakani, *Microchim. Acta*, 2014, **181**, 865–891.
33 C. T. S. Ching, J. W. Chang, T. P. Sun, H. L. Shieh, C. L. Tsai, H. W. Huang, W. H. Liu, C. M. Liu, W. C. Yeh and J. H. Li, *Sens. Actuators, B*, 2011, **152**, 94–98.
34 W. C. Alvin Koh, M. A. Rahman, E. S. Choe, D. K. Lee and Y. B. Shim, *Biosens. Bioelectron.*, 2008, **23**, 1374–1381.
35 M. Eguilaz, L. Agui, P. Yanez-Sedeno and J. M. Pingarron, *J. Electroanal. Chem.*, 2010, **644**, 30–35.
36 Y. Yang, B. Unnikrishnan and S. Chen, *Int. J. Electrochem. Sci.*, 2011, **6**, 3743–3753.
37 C. Xiang, Y. Zou, L. X. Sun and F. Xu, *Electrochem. Commun.*, 2008, **10**, 38–41.
38 C. Xiang, Y. Zou, L. X. Sun and F. Xu, *Talanta*, 2007, **74**, 206–211.
39 T. M. Hu and S. C. Ho, *J. Med. Sci.*, 2011, **31**, 109–115.
40 H. M. Nassef, L. Civit, A. Fragoso and C. K. O'Sullivan, *Analyst*, 2008, **133**, 1736–1741.
41 M. Aubin-Tam and K. Hamad-Schifferli, *Langmuir*, 2005, **21**, 12080–12084.
42 A. Ramanavicius and A. Ramanaviciene, *Fuel Cells-*, 2009, **9**, 25–36.
43 X. Zhand, H. Ju and J. Wang, *Electrochemical Sensors, Biosensors and their Biomedical Applications*, Elsevier, 2008.
44 H. Liu, H. Yamamoto, J. Wei and D. Waldeck, *Langmuir*, 2003, **19**, 2378–2387.
45 Y. C. Yeh, B. Creran and V. M. Rotello, *Nanoscale*, 2012, **4**, 1871–1880.
46 G. Suarez, C. Santschi, O. J. F. Martin and V. I. Slaveykova, *Biosens. Bioelectron.*, 2013, **42**, 385–390.
47 L. Wang and E. Wang, *Electrochem. Commun.*, 2004, **6**, 49–54.
48 E. Eksin and A. Erdem, *Electroanalysis*, 2014, **26**, 1945–1951.
49 M. Fouladgar, S. Mohammadzadeh and H. Nayeri, *Russ. J. Electrochem.*, 2014, **50**, 981–988.
50 R. Masel, *Principles of adsorption and reaction on solid surfaces*, A Wiley-Interscience Publisher, 1996.
51 C. Y. Liao and J. M. Zen, *Sens. Actuators, B*, 2008, **129**, 896–902.
52 N. F. Atta, A. Galal and S. M. Azab, *Anal. Bioanal. Chem.*, 2012, **404**, 1661–1672.
53 J. R. Requena, M. N. Dimitrova, G. Legname, S. Teijeira, S. B. Prusiner and R. L. Levine, *Arch. Biochem. Biophys.*, 2004, **432**, 188–195.
54 O. Nekrassova, N. S. Lawrence and R. G. Compton, *Talanta*, 2003, **60**, 1085–1095.
55 H. Gao, W. Shen, C. Lu, H. Liang and Q. Yuan, *Talanta*, 2013, **115**, 1–5.